REPORT DOCUMENTATION PAGE

Form Approved OMB No. 0704-0188

1. AGENCY USE ONLY (Leave blank)	2. REPORT DATE	3. REPORT TYPE AND DATES COVERED
	1998	Final Report

4. TITLE AND SUBTITLE

Development of Methods and Experimental Investigation of Ceramic Carbon-Carbon and Other Composite Materials Structural Strength at Ultra-High Temperature

5. FUNDING NUMBERS

F6170897W0118

6. AUTHOR(S)

Nozhnitsky, Y.A., Fishgoyt, A.V., Fedina Y.A., Demidov, A.G., Rozanov, M.A., Cherkasova, S.A.

7. PERFORMING ORGANIZATION NAME(S) AND ADDRESS(ES)

Quality Certification Centre
post address 2. Aviamotornaya St.
Moscow 111250
Russia

8. PERFORMING ORGANIZATION REPORT NUMBER

N/A

9. SPONSORING/MONITORING AGENCY NAME(S) AND ADDRESS(ES)

EOARD
PSC 802 BOX 14
FPO 09499-0200

10. SPONSORING/MONITORING AGENCY REPORT NUMBER

SPC 97-4019

11. SUPPLEMENTARY NOTES

12a. DISTRIBUTION/AVAILABILITY STATEMENT

Approved for public release; distribution is unlimited.

12b. DISTRIBUTION CODE

A

13. ABSTRACT (Maximum 200 words)

This report results from a contract tasking Quality Certification Centre as follows: The contractor will investigate ceramic carbon-carbon and other composite materials to determine structural strength at ultra-high temperatures for various aerospace applications.

14. SUBJECT TERMS

Materials, Structural Materials

15. NUMBER OF PAGES

26

16. PRICE CODE

N/A

17. SECURITY CLASSIFICATION OF REPORT	18. SECURITY CLASSIFICATION OF THIS PAGE	19. SECURITY CLASSIFICATION OF ABSTRACT	20. LIMITATION OF ABSTRACT
UNCLASSIFIED	UNCLASSIFIED	UNCLASSIFIED	UL

Development of Methods and Experimental Investigation of Ceramic, Carbon-Carbon and Other Composite Materials Structural Strength at Ultra-High Temperature.

Nozhnitskiy Y.A., Fishgoyt A.V., Fedina Y.A.,
Demidov A.G., Rozanov M.A.,Cherkasova S.A.
CIAM, Moscow, Russia.

Development of Methods and Experimental Investigation of Ceramic, Carbon-Carbon and Other Composite Materials Structural Strength at Ultra-High Temperature.

Nozhnitskiy Y.A., Fishgoyt A.V., Fedina Y.A.,
Demidov A.G., Rozanov M.A.,Cherkasova S.A.
CIAM, Moscow, Russia.

Introduction

Developed equipment and methods for nonmetallic materials mechanical tests at experimentaly-high temperatures were discussed in the first report. This report is mainly devoted to particular investigation of some metholodical problems of ceramic materials crack-resistance investigations. Some problems of high-temperature test of nonmetallic engine components are briefly discussing too.

1. Investigations of crack-resistance and other mechanical properties of ceramic materials in the 20-1500^{o}C temperature interval.

Reliability of details of ceramic materials significantly depends on their crack-resistance under static and cyclic loads in the range of working temperatures. Along with it large cracks can not exist in ceramic details due to material brittleness but small ones can. As the result of technological defects or due to some hard subject's hitting to the surface (neck).

There are a few methods of determining crack-resistance at normal temperature [1]. They are: indentation fracture (IF); indentation strength (IS); single edge pre-cracked beam (SEPB) and single edge notched beam (SENB).

The most developed method from the methodological point of view is SEPB that is widely used for metallic materials. However, large cracks in real ceramic details can't exist.

The most convenient method is IF that permits to get a large number of results using only one sample. But it doesn't simulate real conditions of loading and can't be used at high temperatures.

IS - method is far closer to the real service conditions' but under its applying some concerns appear:

1. How much a form of the crack resembles that of semicircle, which is suggested in calculated formulas?.
2. If there is a possibility of subcritical crack sub-growth between indenting and bending and during bending itself and what is the rate of it?.
3. Whether eliminating of residual indenting stresses used for K_{IC} calculation takes place under bending high-temperature tests?.
4. Whether indenting cracks are being self-cured under high temperatures?.

So, it's necessary to determine crack resistance by different methods and to compare the results of testing different materials with the aim of choosing a method that can be used for real details calculations.

Ceramic details work under high temperatures in oxidizing environment. So, it's very important to define these materials crack-resistance and strength at the range from normal to maximum working temperatures.

While solving this problem a question of the maximum temperature permissible for using the simplest metallic grips under testing in the air arises. Comparing different metallic materials high temperatures properties permits to consider chromium alloys as a perspective material for grips.

In service conditions ceramic details are subjected to constant and cyclic loads. To estimate these details life-time an information is necessary related to crack-growth rate under static and cyclic loads both for normal and high temperatures. It's desirable to get relevances of the type given below:

$$\frac{d\ell}{dN} = F(\Delta K).$$

With their help it's possible to determine a number of loading cycles up to the beginning of catastrophic fracture.

At present standard equipment enabling determination of small crack growth rate in ceramic samples under cyclic loading isn't available. To receive such a data it's necessary to modernize the equipment for metallic materials. And this work is devoted to the investigation of this task.

2. Methodology of tests and tests results.

2.1 Materials

Properties of ceramics on the base of silicium nitride and carbide and also composite ceramic materials on the base of silicium nitride reinforced with SiC whiskers have been studied.

Materials compositions are described in Table 2.1. Each material is marked by a letter.

Table 2.1.

Compositions of material studied and dimensions of the samples.

№	Marking	Composition	Dimensions of samples
1	A	$SiC+30\%TiB_2$	50x5x3
2	B	$SiC+20\%TiB_2$	50x5x3
3	C	SiC+20%AlN	50x5x3
4	D	SiC+30%AlN	50x5x3
5	E	Si_3N_4	50x5x5
6	F	$Si_3N_4+11\%Al_2O_3+TiN$	50x5x5
7	G	$Si_3N_4+5\%Y_2O_3+2\%Al_2O_3$	50x5x3,4
8	H	$Si_3N_4+5\%Y_2O_3+2\%Al_2O_3+TiN$	50x5x3,4
9	K	Composite $Si_3N_4+Y_2O_3+20\%SiC_W$	50x5x3,5

2.2. Methodology of the tests.

The tests being carried out:

1. Determining hardness - H_V and toughness- K_{1C}^{i} of the materials by IF method.
2. Determining strength three-point bending in the 20 - 1500°C temperatures interval.
3. Determining toughness K_{1C}^{e} by IS method in the 20 - 1400°C temperature interval.
4. Determining toughness K_{1C}^{n} by SENB method in the 20 - 1400°C temperature interval.
5. Determining Young's modulus at normal temperature. This value is included in the calculated formulas of IF and IS - methods.
6. Investigating indented cracks sub-growth during samples maturing and self-curing during sample annealing.
7. Investigating cracks growth kinetics under cyclic and static loading at normal and high temperatures.
8. Electron-microscope investigations

2.2.1. Methodology of determining hardness and toughness by IF - method.

The samples have been polished and indented by Vickers diamond pyramid under loading in the 50 400 н interval. After indenting with the help of optical microscope МВИ - 15У42 dimensions of the indentor imprint diagonal - $2a$ and the length of the cracks going out of the imprint corners have been measured (Fig. 2.1.)

The Hardness was calculated as [2]

$$H_V = 0{,}4636 \frac{P_i}{a^2} \qquad (2.1)$$

Where P_i - indenting loading.

The toughness was calculated as [3]

$$K_{1C}^i = \eta_V^R \sqrt{\frac{E}{H_V}} \frac{P_i}{C^{3/2}} \qquad (2.2)$$

Where E - Young's modulus. For ceramics on the Si_3N_4 base.

$E = 2{,}9 \cdot 10^5$ н/mm^2.

For ceramics on the SiC base Young's modulus was determined additionally.

H_V - hardness,

C - crack depth, equal to it's radius, on assumption that the crack is of a semicircle form,

$\eta_V^R = 0{,}018$ [2].

While indenting a lot of imprints turned out to be unconditioned and a and C couldn't be determined. A number of conditioned imprints varied from 5 to 12 for each loading (for each material).

2.2.2. Determining materials strength.

The strength of a material at normal temperature was determined by three-point bending on the basis (distance between supports) of 20 and 40mm. Loading was conducted in direction of the minimal dimension of the sample, equal to 3-3,5 mm (tab. 2.1).

For high temperature tests (up to 1600^{0}C) a special grip was made of chromium alloy VCh17A (Fig.2.2). The sample was heated up to 1400°C in reflecting furnaces and up to 1500°C in furnaces with heating elements made of lanthanum chromite.

It is known while testing the strength under ceramic samples bending those results are considered to be conditioned that have been obtained using $\frac{\ell}{h} > 10\text{-}14$ (ℓ-distance between supports; h - sample thickness). Nevertheless, our tests on the basis of 20 and 40 mm didn't show a significant difference for all the materials tested. So it wasn't necessary to take into account sheer stresses. The strength was determined as:

$$\sigma_в = \frac{3}{2} \frac{P_C \ell}{в h^2} \qquad (2.3),$$

where P_C - loading at the moment of the sample's failure,

ℓ - distance between the outside supports,

$в$ - width and h - thickness of sample.

So it wasn't necessary to take into account sheer stresses.

2.2.3. Determining toughness by IS method.

The sample was indented under the load of 200 H in the middle of its biggest side. Then it was tested as descriled in section 2.2.2. According to (2.3.) the failure stress- σ_C - was determined.

Toughness was calculated without taking into account indenting residual stresses as:

$$K_C^{вW} = 1{,}26 \sigma_C \sqrt{C}. \qquad (2.4)$$

Coefficient 1,26 was calculated for semi-circle crack according to [4]. The bending toughness was calculated according to the formula [2], where indenting residual stresses were taken into account.

$$K_{1C}^{e}=0{,}59\left(\frac{H}{H_V}\right)^{1/8}(\sigma_C P_i^{1/3})^{3/4} \qquad (2.5)$$

2.2.4. Determining toughness SENB method.

The noth of $\approx 0{,}5\ b$ depth was made by a diamond disk perpendicular to the sample's smallest side. The notch width was about 0,5 mm. Then the samples were subjected to three-point bending. The sample was loaded perpendicular to the smallest side. Methodology of heating and loading was just the same as in section.

2.2.5. Determining Young's modulus.

Young's modulus was determined at normal temperature on a special high stiffness facility «Stark» by static bending under stresses of $0.5\sigma_e - \sigma_e$. About 20-30 samples for every material were tested.

2.2.6. Determining cracks sub growth under samples annealing.

For the part of samples made of materials E,F and G the cracks length was measured immediately, in two hours and in two days after indenting.

To determine the annealing influence to the cracks self-curing they were measured immediately after indenting and also after annealing (1070°C-2 hours).

To determine the annealing influence to materials G and H crack - resistance samples were tested for the following sequences of operations:

1. Without annealing.
2. Indenting - annealing - bending.
3. Annealing - indenting - bending.

Annealing was carried out in the air (1070^{0}C - 2 hours). Heating and cooling down to normal temperature were implemented in furnace.

2.2.7.Investigating crack growth kinetics under cyclic and static loading.

Two facilities were modernized to observe the cracks growth in ceramic samples.

Facility PTK (Fig.2.3) is a modified high-temperature microscope HS-4S, provided with a cyclic loading device that enables to carry out bending tests in a chamber with air, vacuum and controlled atmosphere (possible force - 10-500H). Indenting cracks are observed on the low sample surface. The whole picture is shown on the display by TV - camera. Magnification of optical system amounts to 1000 times. The loading frequency is about 0,1 Hertz. Samples are periodically taken off the tests and are studied at scanning electron microscope JEOL - 35CF and then the tests are renewed.

The facility on the base of a modified microscope ИМАШ-5М (К) is ajusted to analogous tests at high - temperature tests. Its scheme is shown in Fig.2.5.

2.2.8. Electron - microscope investigations.

Microspecimens and fractures of the samples failured were investigated by scanning microscope JEOL -35CF. If necessary, a carbon layer was sprayed on non-conductive ceramics. During these investigations Military Handbook - 790 instructions were used.

2.3.Tests results.

2.3.1.The results of determining Young's modulus.

These results are shown in Table 2.2.

Table 2.2.

Young's modulus of SiC ceramics

Composition	Mar-king	Tests number	E, GPa	ΔE, Gpa	$\frac{\Delta E}{E}$, %	E_{max}, GPa	E_{min}, Gpa
SiC+30%TiB_2	A	32	439	9	2	419	455
SiC+20%TiB_2	B	19	428	17	4	399	451
SiC+20%AlN	C	29	362	31	9	301	399
SiC+30%AlN	D	32	360	12	3	333	375

2.3.2. Materials strength at normal temperature.

The results of determining strength under three - point bending are given in Table 2.3. The samples working surfaces are polished or grinded.

Table 2.3.

Materials strength at normal temperature.

№	Material mark	Surface condition	Strength, $\sigma_в$, MPa	Tests number
1	A	G Al*	330±25	6
2	B	G Al	400±53	13
3	C	G Al	333±50	10
4	D	G Al	382±15	4
5	E	G Al	430±40	6
6	F	G Al	480±90	6
7	F	G Ac	320±10	6
8	G	P Al	900±30	6
9	H	P Al	1040±100	6
10	K	G Al	820±110	6

* -first letter - kind of norking: G - grinding, P - polishing;

second letter - direction of grinding or polishing working marks; Al- along, Ac - across a sample.

2.3.3. Materials hardness and toughness got by different methods at normal temperature.

Values of materials hardness and toughness got by different methods are given in Table 2.4.

In this table P_i- indenting load; H_V - hardness; σ_C - failure stress under indented sample bending; K_{1C}^{i} -toughness under three-point bending, calculated according to (2.4.); $K_C^{вW}$ - failure viscosity, got by three-point bending, calculated on (2.4); $K_{1C}^{в}$ - toughness, calculated according to (2.5); K_{1C}^{n} - toughness got by bending of notched sample.

Table 2.4.

Materials hardness and toughness at normal temperature..

Mate-rial mark	P_i H	H_V, MPa	σ_C, MPa	K_{1C}^{i}, MPa$\sqrt{M}$	$K_C^{вW}$, MPa$\sqrt{M}$	$K_{1C}^{в}$, MPa$\sqrt{M}$	K_{1C}^{n}, MPa$\sqrt{M}$
A	200	12,6±4,7	230±40	9,8±2	3,8±0,6	6,3±1	-
	400	14,2	-	12	-	-	-
	-	-	-	-	-	-	6±0,3
B	50	13±2,	-	6,3±0,6	-	-	-
	100	13,7	-	7±1,3	-	-	-
	200	10,1±2	280±130	6,3±1	5,2±2,2	7,6±2,5	-
	*	12,3±2	-	6,6±1	-	-	-

C	50	12,±0,8	-	6,5±1,3	-	-	-
	100	15,9±0,5	-	5,7±1,6	-	-	-
	150	14,2±0,5	-	5,4±1,3	-	-	-
	200	14,9±,05	200,4±3	5,4±1,3	3,6±0,6	5,7±0,6	-
	300	14,2±,06	0	5,4±0,6	-	-	-
	400	-	-	5,7±0,6	-	-	-
	*	14,2±1,4	-	5,7±1,1	-	-	6,3±0,6
			-				
D	50	10,4±1	-	5,1±0,6	-	-	-
	100	10,9±2,7	-	5,7±1	-	-	-
	200	13,8±1,2	166±23	6±1,9	3±0,4	4,9±0,5	-
	300	16,1±3	-	8,9±2,2	-	-	-
	400	13,4±0,07	-	6,2±2,2	-	-	-
	*	12,9±2,3	-	6,3±1,6	-	-	-
E	100	10±0,6	140±10	7,3±0,5	1,9±0,13	3,2±0,16	-
	200	10,5±0,8	130±6	7,6±0,38	2,1±0,3	3,5±0,13	-
	400	10,8±0,2	116±3	7,6±0,6	2,6±0,3	3,8±0,06	-
	*	10,4±0,6	-	7,3±0,6	2,2±0,4	3,5±0,13	-
G	50	18,9±1,5	-	6±1	-	-	-
	100	16,2±0,9	-	5,7±0,6	-	-	-
	200	15,4±0,5	250±50	6±0,2	4,4±0,3	5,7±0,25	-
	400	21±1	-	6,3±0,5	-	-	-
	*	17,9±2,5	-	6±0,3	-	-	-
H	100	15,6	-	-	-	-	-
	200	14,8	234	7,3±0,6	3,8±0,16	5,4	-
	400	16,6	-	-	-	-	-
	*	15,7±0,9	-	-	-	-	-
K	50	10,7±1,8	-	8,8±0,8	-	-	-
	100	13,4±1,5	-	8,1±1	-	-	-
	150	15,3±1,8	-	8,1±0,6	-	-	-
	200	14,4±0,6	357±40	8±1	3,5±0,5	8,3±0,8	-
	300	15,1±0,7	-	9,3±1	-	-	-
	400	13,7±1,4	-	9±0,6	-	-	-
	*	13,8±1,7	-	8,5±0,6	-	-	-

*Average over all Pi.

2.3.4. Indented cracks sub-growth under samples maturing at normal temperature, cracks self-curing under samples annealing and annealing impact on toughness.

The results of measuring cracks length in different time intervals after indenting of 200 H are given in Table 2.5. Numerator is specified vertical crack, length and denominator is that of horizontal cracks.

Table 2.5.

Cracks length in different time t after indenting

Material mark	№ imprint	Indented crack length, 2C, mm		
		t=0	t=2 hours	t=2 days
1	2	3	4	5
E	1	0,6/0,62	-	0,71/0,63
	2	0,6/0,62	-	0,69/0,67

	3	0,66/0,67	-	0,65/0,68
	average	0,63±0,03	-	0,67±0,03
F	1	0,23	-	0,27
	2	0,235	-	0,22
	3	0,2	-	0,2
	average	0,22±0,02	-	0,23±0,04
G	1	0,34/0,325	0,325/0,325	0,35/0,325
	2	0,33/0,35	0,325/0,350	0,335/0,35
	3	0,36/0,34	0,355/0,325	0,360/0,33
	average	0,34±0,013	0,33±0,014	0,34±0,014

The above given data shows that a significant cracks sub-grouth under samples maturing hasn't been revealed.

The annealing influence to (operating conditions - 1070° houres is given in Table 2.6.

Table 2.6.

Indented cracks length shortening on the sample of H -composition, P_i= 200 H

$2a$, mm	2c before annealing, mm	2c after annealing, mm	Cracks length changing, mm
0,155/0,155	0,395/0,32	0,375/0,27	0,02/0,05
0,155/0,155	0,4/0,365	0,36/0,32	0,04/0,045
0,156/0,164	0,406/0,376	0,36/0,34	0,03/0,02
average	-	-	0,034±0,016

As this table shows, a stable cracks shortening takes place, on the average of 0,03mm.

Changing failure stress and toughness in indented sample (IS) bending by annealing (operating conditions - 1070°C - 2 hour) is given in Table 2.7.

Table 2.7.

Annealing influence (1070^{0}C - 2 hours) to ceramics failure characteristics (Pi=200H)

Compo-sition	Operations sequence	σ_C, MPa	K_{1C}^{e}, MPa$\sqrt{M}$
G	indenting - bending	250±15	6,3±0,0,25
	annealing - indenting - bending	210±40	5,7±0,6
	indenting - annealing - bending	310±45	7,6±0,6
H	indenting - bending	234	6,0
	annealing - indenting - bending	260±10	6,6±0,3
	indenting - annealing - bending	590±20	12±0,3

The results show that annealing after indenting raises failure stress and toughness. In case of G-composition this rise is about 25%, and in case of H - composition - about 150%.

2.3.5.Materials strength and crack resistance relationship to temperature.

The results of measuring strength in temperature range between 20°C and 1500°C are given in table 2.8. and in fig. 2.6, 2.8, 2.10, 2.12, 2.14.

Table 2.8.

Materials strength - temperature relationship.

Material mark	$\sigma_в$, MPa					
	20^0C	700^0C	1000^0C	1300^0C	1400^0C	1500^0C
A	330±25	260±10	170±60	-	190±1	-
B	400±50	-	-	230±1	2	-
C	333±50	-	380±120	6	-	225
D	380±15	-	520±50	-	230±3	250
				-	0	
					410	

The results of measuring materials crack-resistance in temperature range between 20^0C and 1400^0C are given in Tables 2.9-2.12 and Fig.2.7, 2.9, 2.11, 2.13, 2.15.

Table 2.9.

Relation of indented samples failure stress under load of 200 H to temperature.

Material mark	σ_C, MPa					
	20^0C	700^0C	1000^0C	1200^0C	1300^0C	1400^0C
A	230±40	200±30	190±30	150±30	160±30	170±30
B	280±130	200	170±20	170±20	160	180±20
C	204±30	278±7	291±40	-	210±40	290±90
D	170±20	220±30	240±60	220±25	230±50	240±20
K	360±40	265±20	290±35	-	390±10	-

Table 2.10

$K_C^{вW}$ values at different temperatures

Material mark	$K_C^{вW}$, MPa$\sqrt{M}$					
	20^0C	700^0C	1000^0C	1200^0C	1300^0C	1400^0C
A	3,8±0,6	3,2±0,6	3,2±0,5	2,5±0,3	2,5±0,5	2,8±0,5
B	5,1±2,2	3,8	3,2±0,3	3,2±0,3	2,8	3,3±0,3
C	3,6±0,6	5,1±0,13	5,1±0,6	-	3,8±0,6	5,4±1,6
D	3±0,4	4,1±0,5	4,4±1	4,1±0,4	4,1±1	4,4±0,3
K	4,4±0,5	3,3±0,25	3,6±0,4	-	4,7±0,13	-

Table 2.11

$K_{1C}^{в}$ values at different temperatures

Material mark	$K_{1C}^{в}$, MPa$\sqrt{M}$					
	20^0C	700^0C	1000^0C	1200^0C	1300^0C	1400^0C
A	6,3±1	5,7±0,6	5,7±0,6	4,7±0,5	5,1±0,5	5,1±0,6
B	7,6±2,5	6	5,1±0,5	5,1±0,5	5,1	5,4±0,5
C	5,7±0,6	7,1±0,13	7,3±0,6	-	5,7±0,8	7,4±1,6
D	4,9±0,5	6,2±0,6	6,5±1,3	6±0,6	6,3±1	6,6±0,3
K	8,2±0,6	6,6±0,3	7,3±0,6	-	8,9±0,2	-

Table 2.12

Notched samples of A- material toughness values at different temperatures.

Temperature, ^{0}C	20	1000	1320	1400
K_{1C}^n, MPa$\sqrt{M}$	6±0,3	6±0,3	5,1	3,3±0,6

2.3.6. Indented cracks growth kinetics under cyclic and static loading.

Investigating cracks growth kinetics has been carried out at G- and H- ceramics and K-composite. Cracks length relationship to the loading cycles number are given in Fig.2,19-2.31. Under static loading with stress equal to the maximum cycle load, cracks growth hasn't been observed.

The most part of the results has been got at a PTK - facility at normal temperature. ИМАШ 5M(K) - facility was put into explotation later and only one test relation has been determined with its help, and it doesn't much differ from those of determined at normal temperature (Fig.2.31).

2.3.7. Electron-microscope investigations.

Structure of A, B, C, D ceramics and K - composite are given in Fig. 2.32 a-d. Fractures of H - material tested by three - point bending are shown in Fig 2.33 a (without indenting) and in Fig.2.33b(without indenting).

2.4. Analysing the results.

2.4.1. Normal temperature tests.

The results of determining Young-modulus (Table 2.2) show that ceramics on the SiC - base with TiB_2 - additives have a higher modulus than those with AlN - additives.

Ceramics strength is shown in Table 2.3. As it was supposed, the surface condition, in particular, marks direction after grinding, has a great in influence the strength limit.

It's also important that the results of determining toughness by different methods, are similar for B,C,G,H and K - ceramics. At the same time K_{1C}^i and K_{1C}^e - values for A,D,E and F - materials differ significantly . The reasons are not clear. It should be stressed that the spread of the results for the materials on SiC - base is wider than for those on Si_3N_4 -base. It can be probably explainned by a significant micro - inhomogeniti of the tested SiC - based ceramics.

During maturing after indenting (Table 2.5.) the crack sub - growth isn't observed. Annealing G - ceramic after indenting leads to some crack length decreasing (Table 2.6.), but it doesn't influence very much to toughness (K_{1C}^e is increasing from 6,3 to 7,6 MPa$\sqrt{M}$).

For H - ceramic the same annealing leads to a significant increase in toughness K_{1C}^e (Table 2.7.) from 6 to 12 MPa$\sqrt{M}$. This K_{1C}^e - increase may be the result of a more intensive crack self-curing comparing with G - ceramic, more complete removing residual stresses or both these phenomenons.

Probably it would be reasonable to investigate increasing ceramic details reliability by the annealing at a possible later of these details manufacturing or design assembly.

2.4.2. High temperature tests.

For A and B materials strength limit, failure stress σ_C and toughness are decreasing relatively monotonously along with temperature increase (Fig. 2.6 - 2.9.).

For C and D materials strength limit has its maximum at about 1000°C, and failure stress σ_C and toughness have their minimum at about 700°C (Fig.2.14, 2.15). Perhaps, the material behavior is influenced by several processes. Along with temperature increasing: strength decreasing, plasticity increasing and surface cracks curing. It's true both for samples with indenting cracks and samples used for determining their strength, as failure stress is determined not only by materials properties but by surface defects as well (mechanical treatment marks, micro - cracks and so on).

2.4.2. High temperature tests.

For A and B materials strength limit, failure stress σ_C and toughness are decreasing relatively monotonously along with temperature increase (Fig. 2.6 - 2.9.).

For C and D materials strength limit has its maximum at about 1000°C, and failure stress σ_C and toughness have their minimum at about 700°C (Fig.2.14, 2.15). Perhaps, the material behavior is influenced by several processes. Along with temperature increasing: strength decreasing, plasticity increasing and surface cracks curing. It's true both for samples with indenting cracks and samples used for determining their strength, as failure stress is determined not only by materials properties but by surface defects as well (mechanical treatment marks, micro - cracks and so on).

Strength limits comparison (Fig.2.16) shows some D - material advantage. Though indented sample σ_C failure stress and toughness at normal and working temperatures (1000 - 1400^{0}C) turn out to be higher for ceramic composite - K (Fig. 2.17,2.18).

2.4.3. Crack growth rate.

Jumping character of cracks growth (Fig.2.19 - 2.31) also draws attention. The crack remains unmovable or quickly covers a distance of 0,01-0,1 mm and then stops again. Perhaps, such character of cracks propagation witnesses that there are some local inhomogeneities with the size of 0,01 -0,1 mm and this is quite larger than the size of the sintered particles which are close to 1-5 mkm (Fig.2.32).

In order to get relationships of cracks rate $d\ell / dN$ and stress intensity coefficient it was necessary to smooth the curve $d\ell / dN = f(N)$, and after that graphical differentiation was implemented. It was, certainly, connected with some subjective point of view. Kinetic diagrams $d\ell / dN = f(\Delta K)$ are shown in Fig.2.34, 2.35. It can be seen that these curves are of one and the same form with minimum at intermediate ΔK. It was supposed that a high crack rate at low ΔK can be explained by large residual stresses due to indenting. These stresses influence is as higher as cracks length lower.

2.4.4.Electron - microscope investigation.

Microstructure of the materials tested is given in Fig. 2.3.2. a-d. A and B materials have larger grain sizes and significant structure in homogeneity in comparison of C - and D- materials. A - material has a visible porosity.

K - material has Si_3N_4 - matrix and light Y_2O_3 - grains. Reinforcing SiC whiskers are observed in matrix, too.

Fractures of samples without indenting have got rough surface. As a rule, the fracture began from the sample corner (Fig.2.33a). Fracture surface after indenting is smoother. It's easy to see Vikkers - pyramid imprint, initial semi - circle crack and crack which is perpendicular to the fracture and comes from the imprint. The latter is deeper than the initial crack. It means that during sample bending not only the crack perpendicular to load grew, but also the crack parallel to the first did.

3. Component testing.

Monolithic ceramic and composite materials properties observed in actual components can differ significantly from those derived from testpieces due to differences in manufacture technology, reinforcement schemes, scale-factor influence and so on. This is a reason why tests of components made of high-temperature nonmetallic materials are of great importance.

Turbine nozzle vanes, blades and combustion chamber components are usually tested in a high temperature gas flow test rigs [5-8]. These test rigs are shown in Fig 3.1 and Fig 3.2. Thermomechanical fatigue tests also can be carried using high-frequency heating and suspector [9].

Turbine blade and other rotor components are tested in special spin pit rigs and experimental engine cores [6].The spin pit design (Fig. 33) makes it possible to perform spinning of rotor with blades in atmospheric conditions (but not in a vacuum chamber), using friction of rotor-on-air to heat the rotor, as well as by exciting the blades vibrations with the required harmonic with the use of special turbulators. The vibration modes of blades are preliminary investigated with the use of methods of holographic interferometry. To investigate the blade high-cycle fatigue (up to 20KHz, including complicated modes of vibrations) at normal temperature, it is possible apply air vibration benches, where resonance vibrations are excited by a modulated jet of compressed air. During investigation of blade made of hot-pressed ceramic it is necessary to take into account that machining is very expensive and lock-on connection strength significantly influences to blade serviceability. So tests in the centrifugal forces field were conducted in several stages. At first stage (before blade airfoil machining), strength of lock-on connection was checked in spin pit, then the completely-mashined blade was tested there. In the absence of failure, the blade was tested in a complete engine gas-generator. Figure 3.4 shows the mounting of specimen and ceramic blade into specially upgraded turbine wheel. During tests centrifugal and temperature loads, number of cycles (idle-take-off- idle) and running time were increased step by step using different turbine wheels and facilities.

Developed methods and equipment were used for tests of different engine components made of ceramic. Carbon-carbon and other composite material. [5-8].

Conclusions.

1. Methods have been developed and experimental investigation has been implemented concerning strength and crack resistance of ceramic based on SiC and Si_3N_4 and ceramic composite with Si_3N_4 matrix and SiC - whiskers at 20 - 1500^{0}C temperature. Toughness was determined by different methods: indentation fracture (IF);indentation strength (IS) and single edge notched beam (SENB).
2. A,B,C - ceramics strength limit decreases along with temperature increasing; D - material has strength maximum at 1000°C. A and B ceramics toughness decreases along with temperature increasing; C and D - ceramics toughness increases; and composite ceramic has its minimum toughness at 700 - 800°C.
3. In has been experimentally shown that using IF and IS - methods for toughness determination gives similar results not for all ceramics. For some ceramics the results obtained by different methods differ significantly.
4. It has been shown that annealing 1070°C - 2 hours after indenting can lead to a substantial increasing failure stress and toughness determined by IS - method.
5. Facilities have been put into exploitation for cyclic testing ceramic samples with direct observing crack growth under cyclic and static loading at normal and high temperatures. Crack growth for G,H - ceramics and K - composite has been investigated.
6. For all materials tested crack growth under cyclic loading has jumps of 0,01 - 0,1 mm length. Relationships of crack growth rate and stress intensity coefficient aren't monotonious and they have minimum at intermediate values ΔK. Cracks growth isn't observed under static loading with a stress equal to maximum stress in cycle, when cracks cyclic propagation takes place.
7. Methods and equipment have been developed and widely used for high-temperature tests of different engine components made of nonmetallic materials.

References.

1. ESIS TS 6 Round Robin on Fracture Toughness. (Draft August 1995) EMPA, Report № 155 088 AUGUST 1995.
2. Lawn, D.B. Marshall. Hardness, Toughness, and Brittleness: An Indentation Fracture Analysis. J.Am. Ceram. Soc., 1979, № 7-8, p.347-350.
3. Lawn, E.R. Faller. Equilibrium Penny-Like Cracks in Indentation Fracture. J.Mat. Sci., 1975, v.10, № 12, p.2016-2024.
4. Broek D. Elementary Engineering Fracture Mechanics Nordhoff International Publishing, Leyden, 1975.
5. Y.Nozhnitsky and L.Smirnov. Ceramic, carbon-carbon and other composite materials tests at high temperature. In «Ultra high temperature mechanical testing», Edited by R.D. Lohr and M.Steen. Woodhead publishing limited, pp 184-192.
6. E.G.Kuznetsov, K.M.Popov, T.D. Karimbaev, L.V.Demidova «Investigation of serviceability of ceramic component for gas turbine engines. Materials of the Seventh Cimtec Word Ceramic Congress. Montecatini Terme (Italy), 1990, pp 73-74.
7. Y.A.Nozhnitsky, L.E. Smirnov, A.S.Marcov, V.N.Sakovich. Experimental Investigation of Ceramic Materials and Turbine Rotor Components. Extending abstracts of the 4-th Int.Symp. on Ceramic Materials and Components of Engines. Goteborg(Sweden)
8. Y.A.Nozhnitsky, Y.A.Fedina, A.D.Rekin, N.I.Petrov Development and investigation of ceramic parts for gas-turbine engines. ASME 97-GT-157, 8p.
9. Y.A.Nozhnitsky, R.A.Doulnev,V.G.Soundyrin Damage Mechanism for thermomechnical fatigue of Aircraft Engines Materials. AGARD CP 569, NATO 1996, pp14.1-14.12

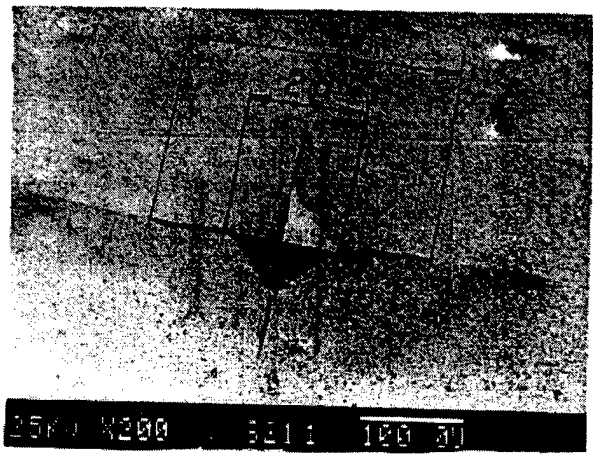

Fig. 2.1. Vickers indentation in composition H ceramics.

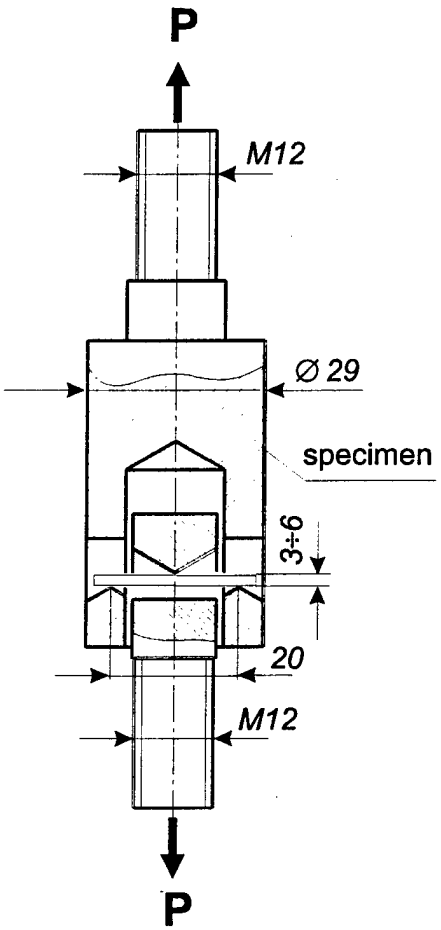

Fig. 2.2 High temperature chrome alloy grip

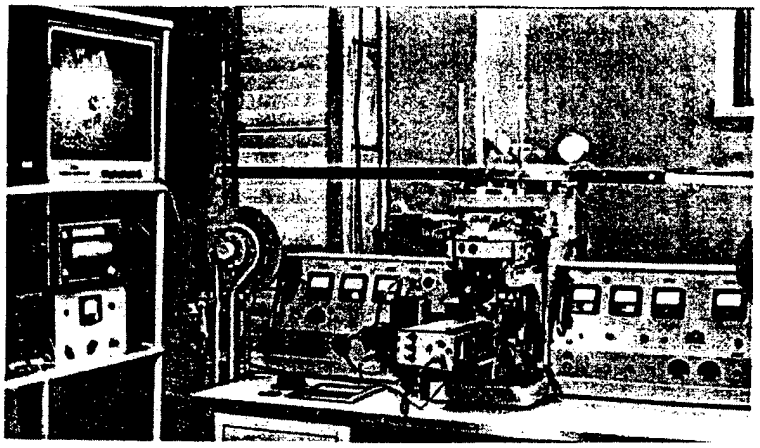

Fig.2.3. Common view PTK apparatus

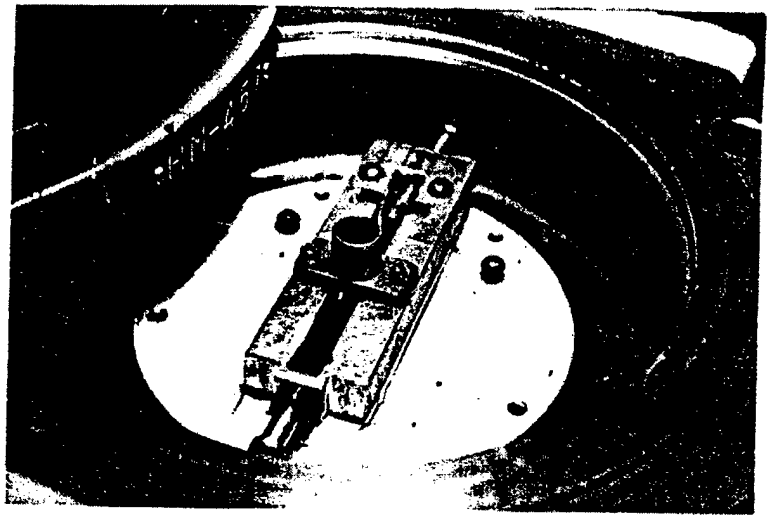

Fig.2.4. Specimens chamber of apparatus PTK

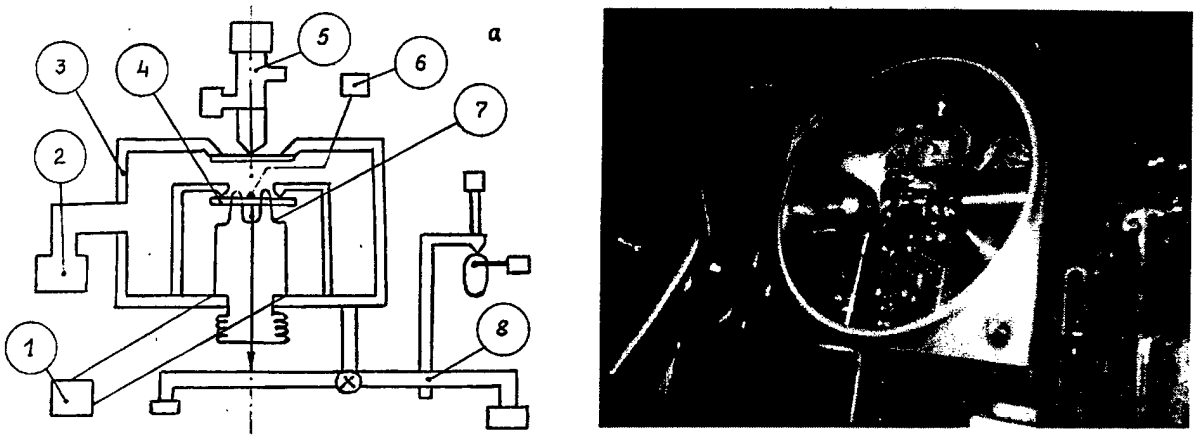

Fig.2.5. Common scheme - a and specimens chamber of ИМАШ-5М(К) apparatus.

1. - Temperature support system
2. - Vacuum system
3. - Specimens chamber
4. - Specimen
5. - Microscope with TV
6. - Temperature measuring system
7. - Heater
8. - Loading system

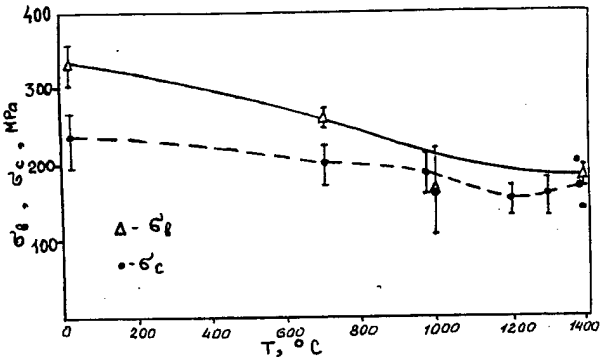

Fig.2.6. Ultimate strength and indenting specimens fracture stress of material A.

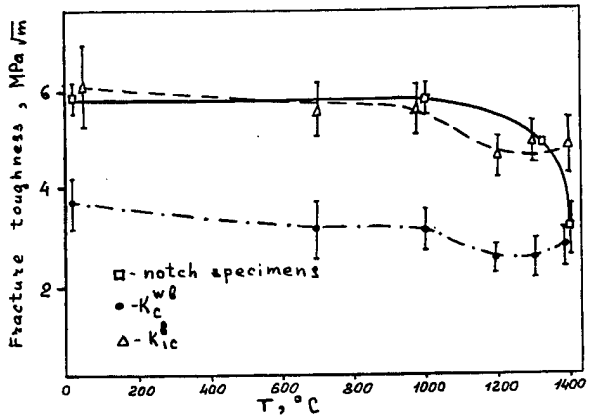

Fig.2.7.Fracture toughness volumes of A material, calculated on formula (2.4) - K_c^{bw}, (2.5)- K_{1c}^{b} and received on the notched specimens.

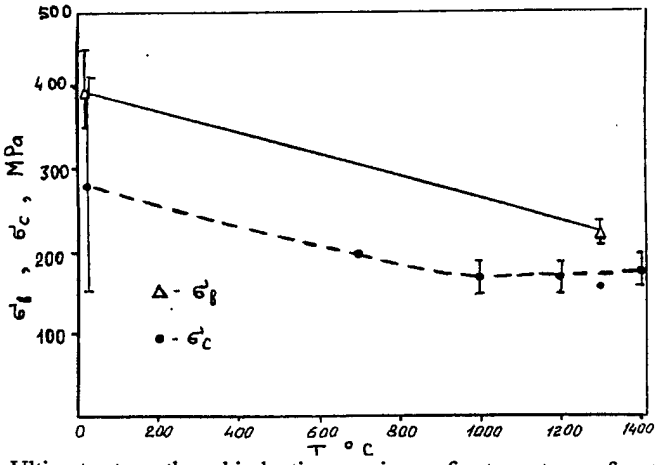

Fig.2.8. Ultimate strength and indenting specimens fracture stress of material B.

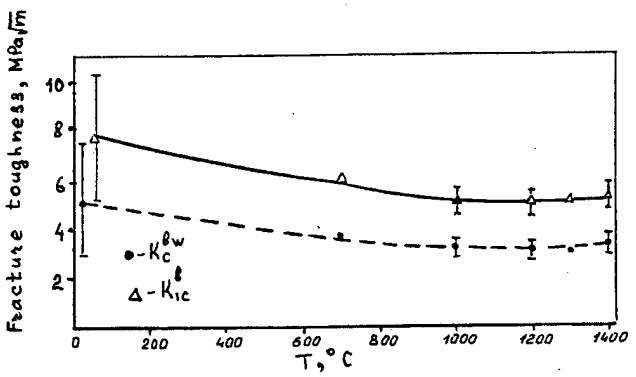

Fig.2.9. Fracture toughness volumes of B-material calculated on formula (2.4) - K_c^{bw} ,(2.5)- K_{1c}^{b}.

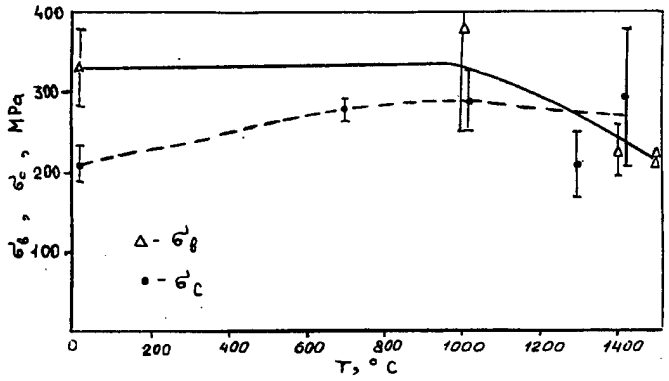

Fig.2.10. Ultimate strength and indenting specimens fracture stress of material C.

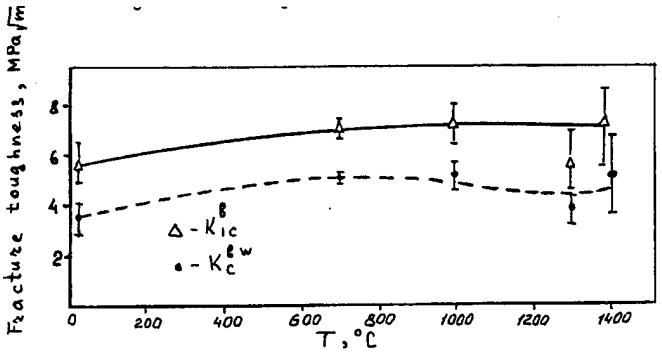

Fig.2.11. Fracture toughness volumes of C-material, calculated on formula (2.4) K_c^{bw}, (2.5) K_{1c}^{b}

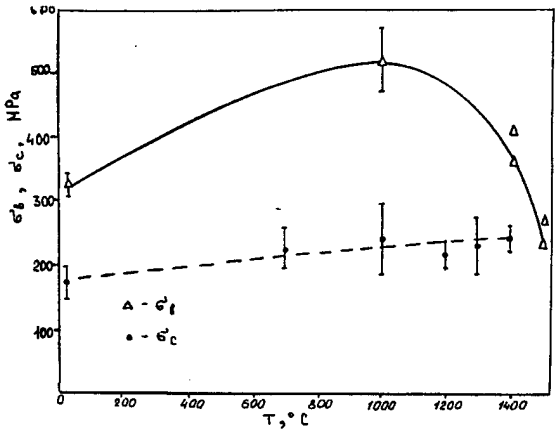

Fig.2.12 Ultimate strength and indenting specimen fracture stress of material D.

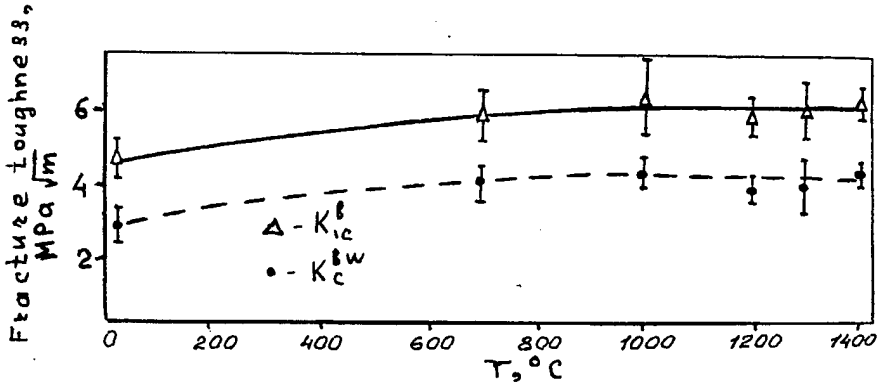

Fig.2.13.Fracture toughness volumes of D-material, calculated on formula (2.4) - K_c^{bw} and (2.5) - K_{1c}^{b}

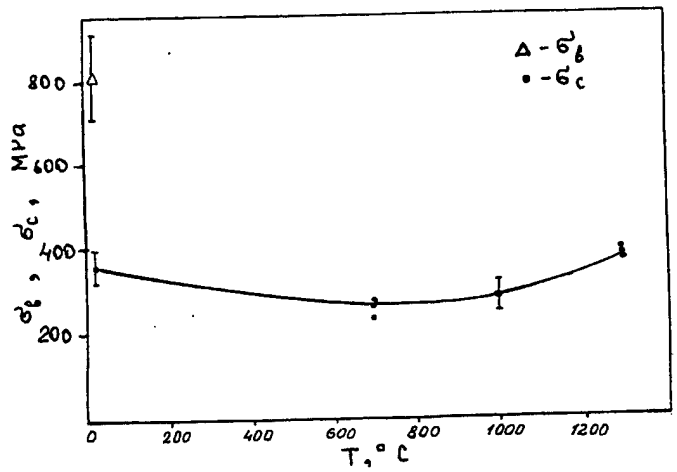

Fig.2.14. Ultimate strength and indenting specimens fracture stress of composite K.

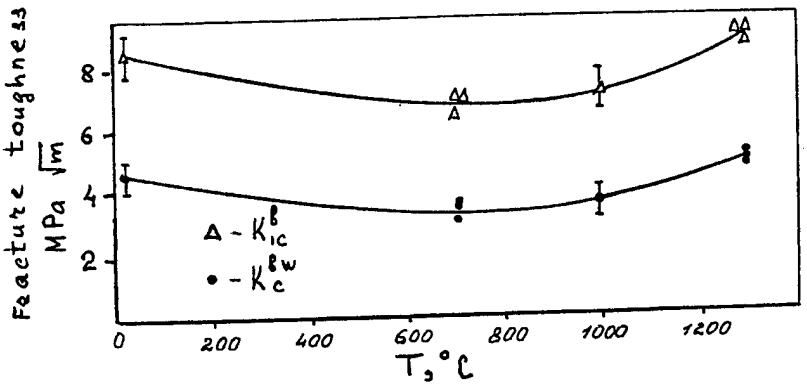

Fig.2.15. Fracture toughness volumes of composite calculated on formula (2.4) - K_c^{bw} and (2.5) - K_{1c}^{b}.

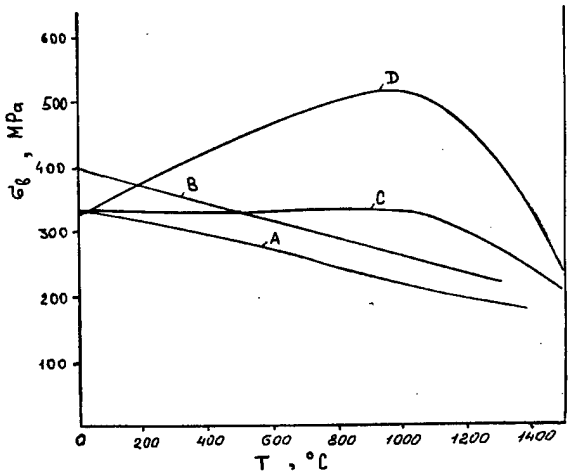

Fig.2.16. Comparison of ultimate strength of different materials.

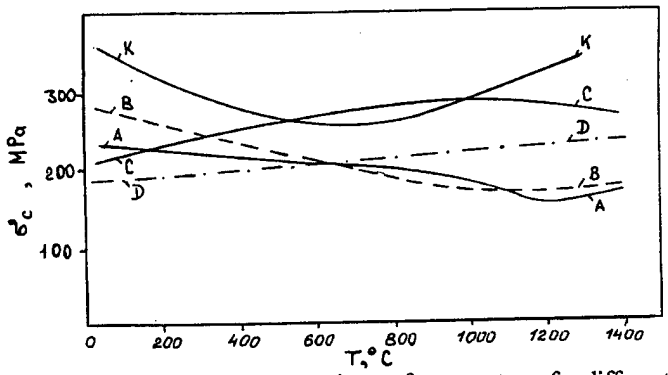

Fig.2.17. Comparison of indentation specimens fracture stress for different materials.

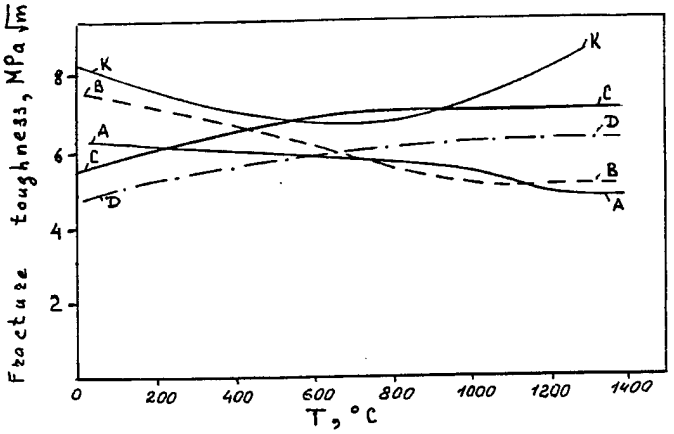

Fig.2.18. Comparison of fracture toughness (K_{1c}^{b}) volumes for different materials.

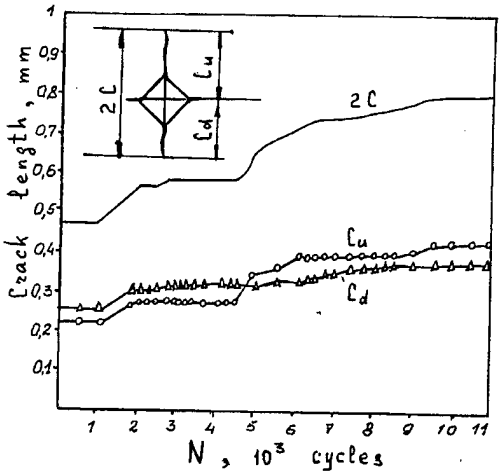

Fig. 2.19. Crack growth in ceramics G
P_i=200N, σ_{max} =187MPa.

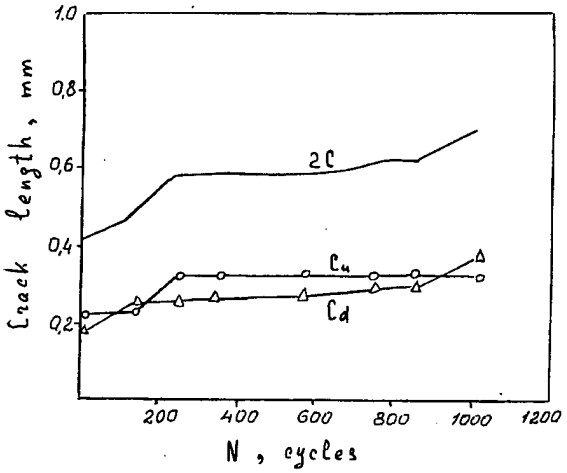

Fig.2.20. Crack growth in ceramics G
P_i=200N, σ_{max} =187MPa.

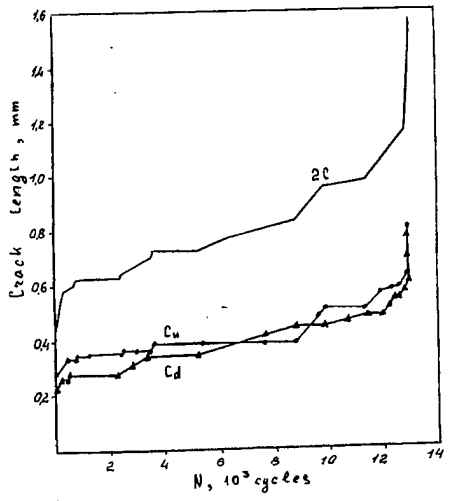

Fig.2.21.Crack growth in ceramics G
P_i=200N, σ_{max} =208MPa.

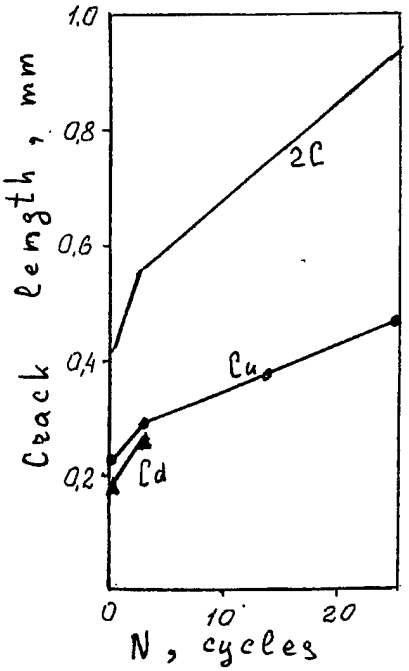

Fig.2.22. Crack growth in ceramics G
P_i=200N, σ_{max}=218MPa.

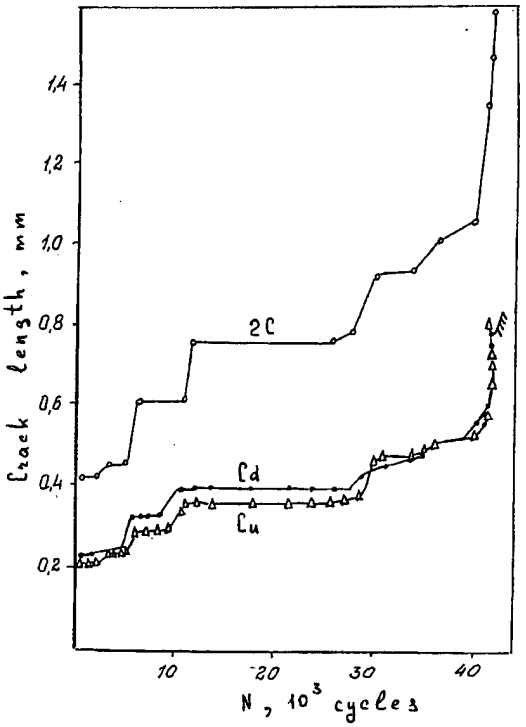

Fig.2.23. Crack growth in ceramics H
P_i=200N, σ_{max}=187MPa.

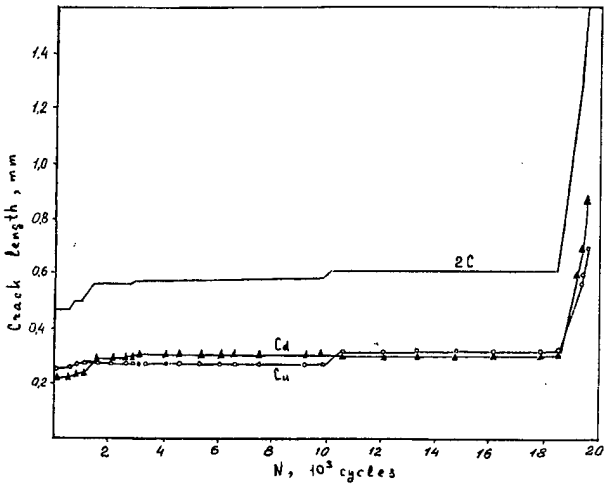

Fig.2.24. Crack growth in ceramics H
P_i=200N, σ_{max}=187MPa.

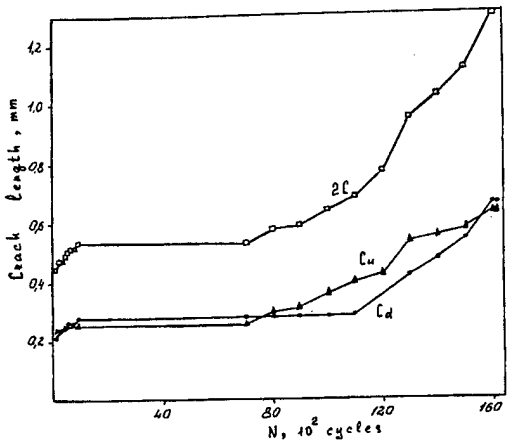

Fig. 2.25. Crack growth in ceramics H
P_i=200N, σ_{max}=218MPa.

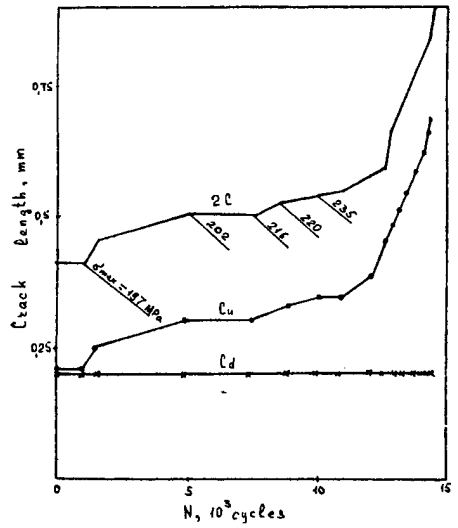

Fig.2.26. Crack growth in composite K
P_i=200N, σ_{max} is indicated on the curves.

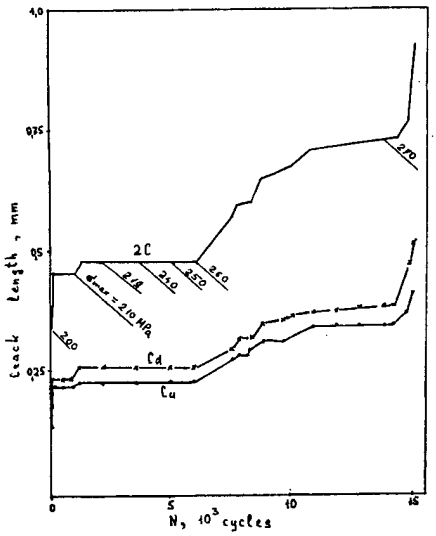

Fig.2.27. Crack growth in composite K
P_i=200N, σ_{max} is indicated on the curves.

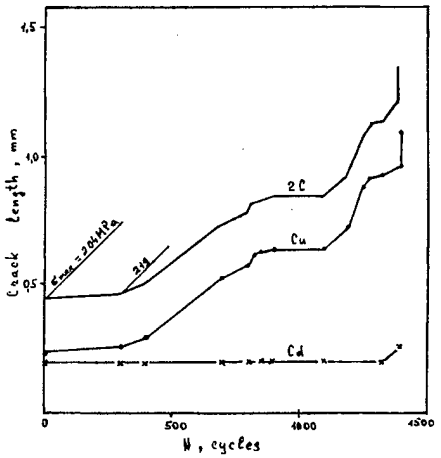

Fig.2.28. . Crack growth in composite K
P_i=200N, σ_{max} is indicated on the curves.

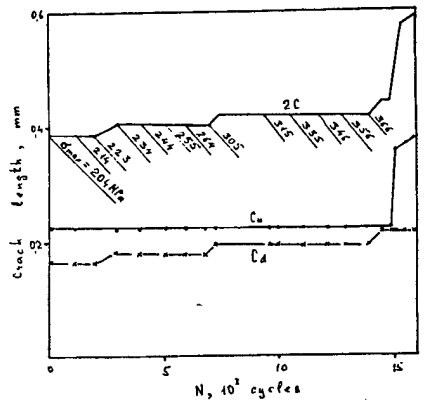

Fig.2.29. . Crack growth in composite K
P_i=200N, σ_{max} is indicated on the curves.

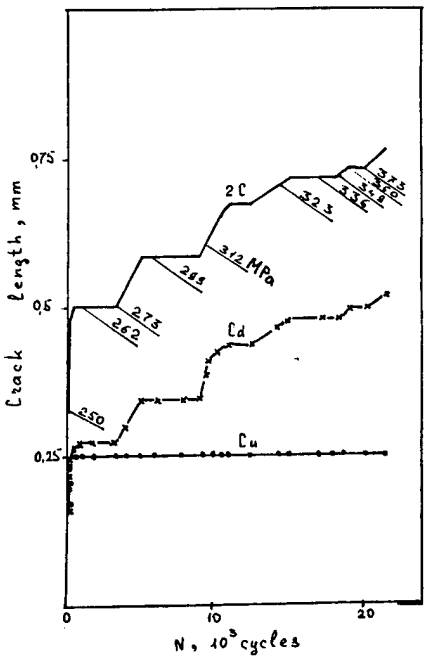

Fig.2.30. . Crack growth in composite K
P_i=200N, σ_{max} is indicated on the curves.

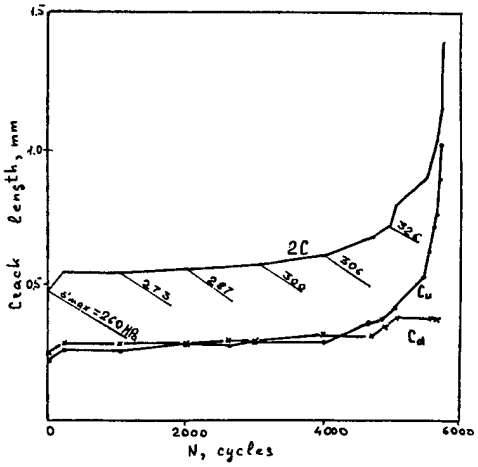

Fig.2.31. . Crack growth in composite K
P_i=200N, σ_{max} is indicated on the curves.

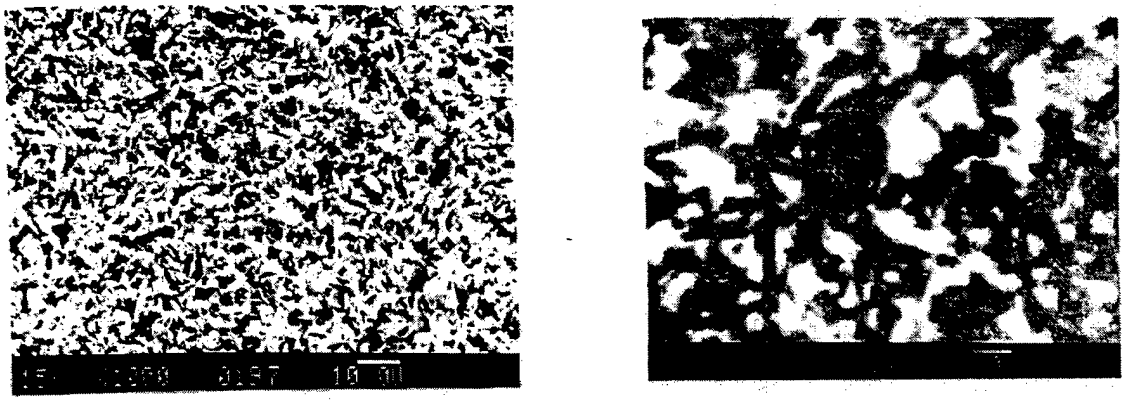

Fig.2.32. Microstructure of ceramics A-a, B-b, C-c, D-d and composite K-e

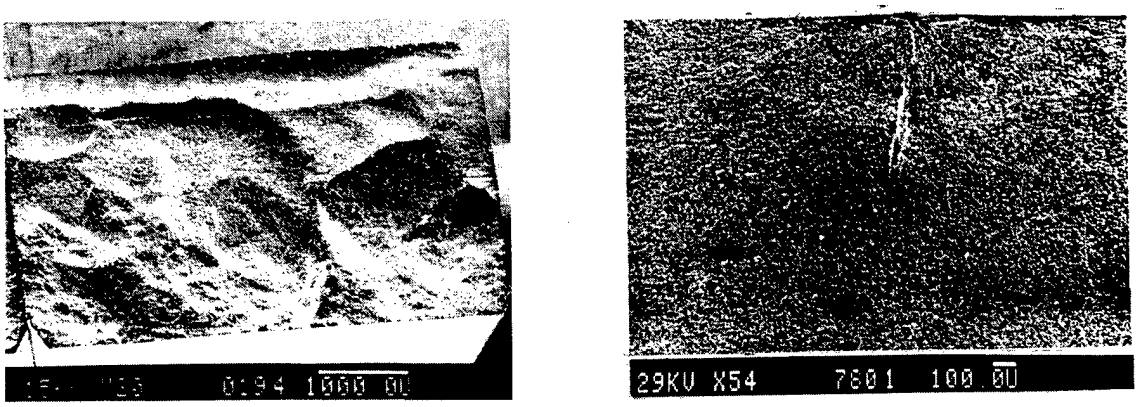

Fig.2.33. Fracture surface of ceramics H:
a. Bending without indentation.
b. Bending after indentation.

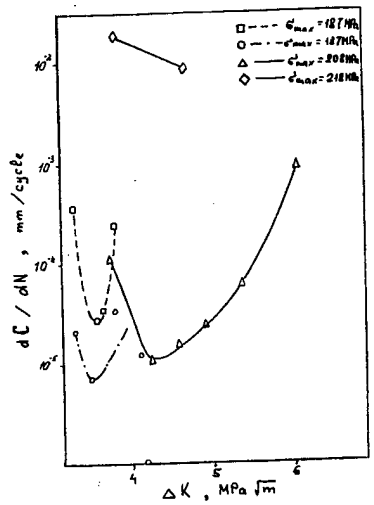

Fig.2.34. Cracks rate as a function of stress intensity factor on ceramics G.

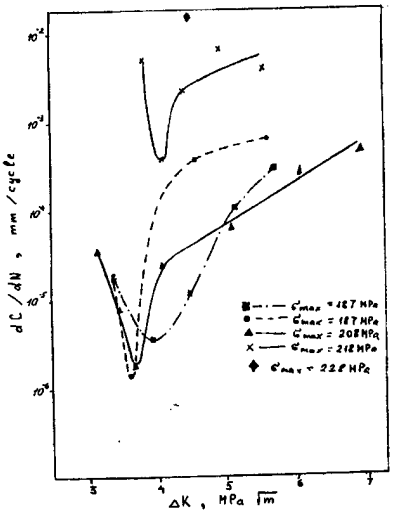

Fig.2.35. Cracks rate as a function of stress intensity factor on ceramics G.

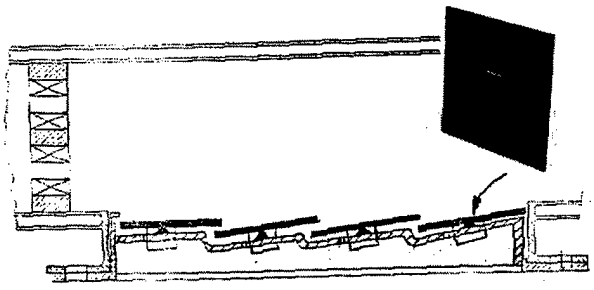

Fig 3.1 Experimental combustion chamber with ceramic segments.

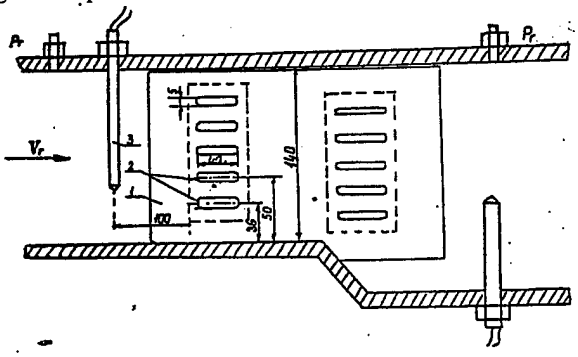

Fig 3.2. Termocicling of nozzle vanes and blades

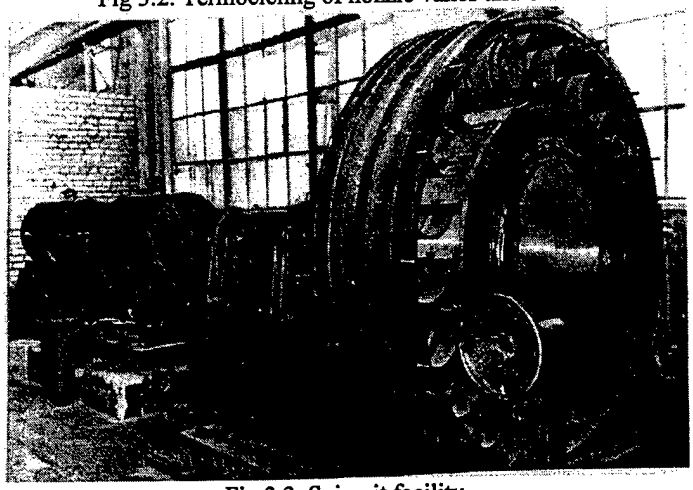

Fig 3.3 Spin pit facility.

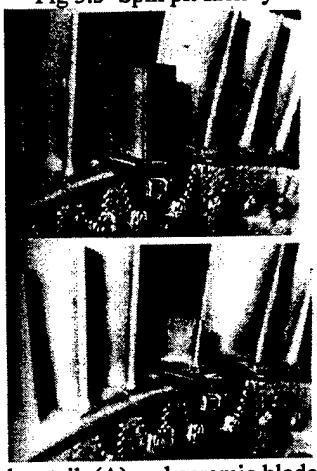

Fig 3.4 Mounting of specimen machined dovetail (A) and ceramic blade (B) into specially upgraded turbine wheel